Early Optical Polarization of a Gamma-Ray Burst Afterglow

Carole G. Mundell, *et al.*

Science **315**, 1822 (2007);
DOI: 10.1126/science.1138484

Science (print ISSN 0036-8075; online ISSN 1095-9203) is published weekly, except the last week in December, by the American Association for the Advancement of Science, 1200 New York Avenue NW, Washington, DC 20005.

18. K. E. Gottschalk, *Structure* **13**, 703 (2005).
19. A. Senes *et al.*, *J. Mol. Biol.* **366**, 436 (2007).
20. M. Lopez de la Paz, L. Serrano, *Proc. Natl. Acad. Sci. U.S.A.* **101**, 87 (2004).
21. Y. Huang, M. J. Lemieux, J. Song, M. Auer, D. N. Wang, *Science* **301**, 616 (2003).
22. P. Jordan *et al.*, *Nature* **411**, 909 (2001).
23. D. Gerber, N. Sal-Man, Y. Shai, *J. Biol. Chem.* **279**, 21177 (2004).
24. J. M. Harris, N. E. Martin, M. Modi, *Clin. Pharm.* **40**, 539 (2001).
25. A. Z. Ebie, K. G. Fleming, *J. Mol. Biol.* **366**, 517 (2007).
26. R. Fairman *et al.*, *Proc. Natl. Acad. Sci. U.S.A.* **90**, 10429 (1993).
27. W. P. Russ, D. M. Engelman, *Proc. Natl. Acad. Sci. U.S.A.* **96**, 863 (1999).
28. D. Langosch, B. Brosig, H. Kolmar, H. J. Fritz, *J. Mol. Biol.* **263**, 525 (1996).
29. D. Gerber, N. Sal-Man, Y. Shai, *J. Mol. Biol.* **339**, 243 (2004).
30. S. Kim *et al.*, *Proc. Natl. Acad. Sci. U.S.A.* **102**, 14278 (2005).
31. R. I. Litvinov, H. Shuman, J. S. Bennett, J. W. Weisel, *Proc. Natl. Acad. Sci. U.S.A.* **99**, 7426 (2002).
32. R. I. Litvinov, G. Vilaire, H. Shuman, J. S. Bennett, J. W. Weisel, *J. Biol. Chem.* **278**, 51285 (2003).
33. A. Senes, D. E. Engel, W. F. DeGrado, *Curr. Opin. Struct. Biol.* **14**, 465 (2004).
34. K. R. MacKenzie, J. H. Prestegard, D. M. Engelman, *Science* **276**, 131 (1997).
35. D. M. Engelman *et al.*, *FEBS Lett.* **555**, 122 (2003).
36. A. K. Doura, K. G. Fleming, *J. Mol. Biol.* **343**, 1487 (2004).
37. A. Senes, I. Ubarretxena-Belandia, D. M. Engelman, *Proc. Natl. Acad. Sci. U.S.A.* **98**, 9056 (2001).
38. L. Adamian, J. Liang, *Proteins* **47**, 209 (2002).
39. B. H. Luo, C. V. Carman, J. Takagi, T. A. Springer, *Proc. Natl. Acad. Sci. U.S.A.* **102**, 3679 (2005).
40. K. L. Wegener *et al.*, *Cell* **128**, 171 (2007).
41. A. W. Partridge, R. A. Melnyk, D. Yang, J. U. Bowie, C. M. Deber, *J. Biol. Chem.* **278**, 22056 (2003).
42. N. Manolios *et al.*, *Nat. Med.* **3**, 84 (1997).
43. D. Gerber, F. J. Quintana, I. Bloch, I. R. Cohen, Y. Shai, *FASEB J.* **19**, 1190 (2005).
44. H. Yin *et al.*, *J. Biol. Chem.* **281**, 36732 (2006).
45. L. L. Freeman-Cook *et al.*, *J. Mol. Biol.* **338**, 907 (2004).
46. We acknowledge NIH (grants GM60610, HL40387, HL54500, and GM54616) and NSF (grant 050020) for support of this work. We also received training grants from NIH (5T32 CA101968 and 5T32 GM08275) and NSF (DMR03 04531). We thank R. Gorelik for preliminary studies into DN-TOXCAT assays.

Supporting Online Material

www.sciencemag.org/cgi/content/full/315/5820/1817/DC1
Materials and Methods
Figs. S1 to S9
Tables S1 and S2
References

26 October 2006; accepted 16 February 2007
10.1126/science.1136782

REPORTS

Early Optical Polarization of a Gamma-Ray Burst Afterglow

Carole G. Mundell,[1]* Iain A. Steele,[1] Robert J. Smith,[1] Shiho Kobayashi,[1] Andrea Melandri,[1] Cristiano Guidorzi,[1,2,3] Andreja Gomboc,[4] Chris J. Mottram,[1] David Clarke,[5] Alessandro Monfardini,[1,6] David Carter,[1] David Bersier[1]

We report the optical polarization of a gamma-ray burst (GRB) afterglow, obtained 203 seconds after the initial burst of γ-rays from GRB 060418, using a ring polarimeter on the robotic Liverpool Telescope. Our robust (2σ) upper limit on the percentage of polarization, less than 8%, coincides with the fireball deceleration time at the onset of the afterglow. The combination of the rate of decay of the optical brightness and the low polarization at this critical time constrains standard models of GRB ejecta, ruling out the presence of a large-scale ordered magnetic field in the emitting region.

Gamma-ray bursts are the most instantaneously powerful explosions in the universe and represent the most important new astrophysical phenomenon since the discovery of quasars and pulsars. Identified as brief, intense, and unpredictable flashes of high-energy γ-rays on the sky, the most common type of GRB, so-called long bursts, have γ-ray pulses that last longer than 2 s. These are thought to be produced when a massive star reaches the end of its life, its core collapsing to form a black hole and, in the process, ejecting an ultrarelativistic blastwave (*1*, *2*). In many cases, the detected γ-ray flux implies an unphysically high explosion energy if assumed to be emitted isotropically by the source, the so-called energy catastrophe. Instead, focusing the energy into a narrow jet reduces the intrinsic energy output to a canonical $\sim 10^{51}$ erg for most GRBs (*3*).

After the initial burst of γ-rays, the subsequent radiation produced at longer wavelengths (e.g., x-ray, optical, or radio), termed the "afterglow," is generally accepted to be synchrotron radiation whose observed properties are consistent with a focused jet expanding at ultrarelativistic speeds into the interstellar medium. The production of synchrotron radiation requires the presence of a magnetic field, but the origin and role of the magnetic fields in GRB ejecta are a long-standing open issue. In turn, fundamental questions on the driving mechanism of the explosion, in particular, whether the relativistic outflow is dominated by kinetic (baryonic) or magnetic (Poynting flux) energy, remain unanswered (*4*, *5*). The primary challenges in addressing these issues arise because GRBs are short-lived, compact, and lie at vast cosmological distances; our understanding of their physical nature is therefore inferred from the characteristics of their radiation, measured at the earliest possible time when the observed radiation is still sensitive to the properties of the original fireball.

The two main models of collimated relativistic outflows, or jets, that have been proposed are the hydrodynamical and the magnetized jet (*5*). Hydrodynamical jets have no dominant ordered magnetic field but instead produce synchrotron radiation from tangled magnetic fields, concentrated in the thin layer of the expanding shock front, that are generated locally by instabilities in the shock (*6*); the magnetic field does not influence the subsequent evolution of the jet. Models of these jets have been highly successful at reproducing a wide range of observed properties of GRBs (*1*, *2*). A relativistic outflow from a central engine might have a weak ordered or random magnetic field. As long as the magnetic field does not affect the dynamics of the jet, we classify it as a hydrodynamical jet. In contrast, magnetized jets are threaded with strong, globally ordered magnetic fields, which originate at the central source, are advected outward with the expanding flow, and may provide a powerful mechanism for collimating and accelerating the relativistic jet (*7*, *8*). A magnetic driving mechanism is an attractive scenario to account for the prodigious energy outputs and vast accelerations required for GRB ejecta, as well as for overcoming energy-efficiency problems inherent in hydrodynamical models in which internal shocks must convert kinetic energy to radiative energy with sufficient efficiency to produce the observed γ-ray emission and prolonged central engine activity (*9*, *10*).

Observationally, the fading rate of the afterglow emission alone is inadequate as a diagnostic for distinguishing between these theoretical jet models (*11*–*13*); in contrast, the polarization

[1]Astrophysics Research Institute, Liverpool John Moores University, Twelve Quays House, Egerton Wharf, Birkenhead, CH41 1LD, UK. [2]Dipartimento di Fisica, Universitá di Milano-Bicocca, Piazza delle Scienze 3, 20126 Milano, Italy. [3]Istituto Nazionale di Astrofisica-Osservatorio Astronomico di Brera, via Bianchi 46, 23807 Merate (LC), Italy. [4]Faculty of Mathematics and Physics, University of Ljubljana, Jadranska 19, 1000 Ljubljana, Slovenia. [5]Department of Physics and Astronomy, University of Glasgow, Glasgow G12 8QQ, UK. [6]CNRS, Institut Néel, 25 Avenue des Martyrs, 38042 Grenoble, France.

*To whom correspondence should be addressed. E-mail: cgm@astro.livjm.ac.uk

properties are predicted to differ markedly. Observations of the polarization state of GRB afterglow emission therefore offer a diagnostic to eliminate or constrain current models. The testable prediction is that hydrodynamical jets produce a considerable amount of polarization at the geometrical transition phase a few days after the burst, the so-called jet break time when the lateral spreading of the slowing jet produces a characteristic steepening of the light curve, and produce little or no polarization at early times, whereas jets with large-scale globally ordered magnetic fields produce polarization substantially greater than 10% at early times (*12*, *13*) and in some cases as high as ~50% (*13*).

The first detection of polarized optical emission from a GRB afterglow was taken at 0.77 days after the burst of GRB 990510 and, with the exception of GRB 020405 for which an unexplained high degree of optical polarization was measured 1.3 days after the burst (*14*), late-time measurements of optical polarization for other long bursts taken typically at $t \gtrsim 0.2$ day all show consistently low values of $P \sim 1$ to 3%, some of which may be induced by interstellar scattering processes (*15*–*18*). Although these painstaking observations of late-time polarization were vital in confirming the presence of collimated jets in GRBs [e.g., (*15*–*17*)], there was a lack of polarization observations of GRB afterglows in the early phase within the first few minutes, where the predicted properties of magnetized or unmagnetized hydrodynamic jets differ most.

Recent advances in technical efficiency of catching the rapidly fading light from GRBs, driven primarily by the real-time dissemination of accurate localizations of GRBs discovered by the Swift satellite (*19*), have opened a new era in rapid-response follow-up studies of GRBs and their afterglows (*1*, *2*).

GRB 060418 was detected by the Swift satellite at 03:06:08 UT on 18 April 2006 and exhibited a triple-peaked γ-ray light curve with overall duration of ~ 52 s, followed by a small bump at 130 s coincident with a large flare detected in the x-ray light curve and likely associated with ongoing central engine activity (*20*). A localization was communicated automatically to ground-based facilities and triggered robotic follow-up observations at the 2.0-m Liverpool Telescope in La Palma, the Canary Islands. These observations consisted of a 30-s exposure with the RINGO polarimeter (Fig. 1) beginning at 03:09:31 UT or 203 s after the start of the prompt γ-ray emission and contemporaneous with the fading tail of this γ-ray emission, followed by 2 hours of multicolor photometric imaging. We concentrate here on the RINGO measurement.

RINGO uses a rotating polaroid to modulate the incoming beam, followed by corotating deviating optics that transform each star image into a ring that is recorded on the charge-coupled device (CCD) chip. Any polarization signal present in the incoming light is mapped out around the ring in a sin(2θ) pattern. A description of the instrument and the data reduction procedures are given in (*21*). A bright star in the field of view of the GRB (Fig. 1) was used as a check on our data reduction, with multiple measurements made on subsequent nights confirming its measured polarization in the GRB frame of <1%. This value also provides a lower limit to any contribution of polarization that could have been induced into the GRB by galactic interstellar dust. No appreciable polarization signal could be detected from the GRB. To quantify this observation, we carried out a Monte Carlo error analysis in an attempt to recover an artificially induced polarization signal with a noise spectrum identical to that of the GRB data. This gave a firm (2σ) upper limit to the measured polarization of <8% [polarizations of 10%, for example, being easily detectable (*21*)].

The optical and near-infrared light curves of GRB 060418 are smooth and featureless; the infrared (IR) light curves show a smooth rise (decay rate $\alpha \sim 2.7$, where $F \propto t^{\alpha}$) to a broad peak at time $t_{peak} \sim 153$ s (*22*) before fading away with a smooth, unbroken power law with $\alpha \sim -1.2$, identical to the decay rate of the optical light curves and typical of standard fireball models of optical afterglows. In the standard GRB fireball model in which a jet is driven into the surrounding circumburst medium, the early afterglow light is thought to include contributions from both a forward shock, which propagates into the ambient medium, and a reverse shock, which propagates back into the original fireball ejecta (*23*). Forward-shock emission peaks when the fireball decelerates or when the typical synchrotron frequency (ν_m) passes through the observed band. The lack of color change around the peak in the IR light curves of GRB 060418 (*22*) confirms the deceleration interpretation, with ν_m already lying below the optical and IR bands at this time (*22*). The steep temporal rise of the IR light curve ($\alpha \sim 2.7$) is also consistent with theoretical predictions of forward-shock emission before deceleration (*24*).

The RINGO measurement was made close to the time of the peak of the IR light curve at the fireball deceleration time and onset of the afterglow, making the polarization measurement particularly important for testing afterglow predictions from current standard jet models. Our polarization measurement also coincides with the decay phase of the x-ray flare emission. Extrapolating the peak flux density in the x-ray flare at 130 s to optical wavelengths, and assuming a spectral index between optical and x-ray bands of $\beta \sim 1$ ($F_\nu \propto \nu^{-\beta}$), we found that the maximum contribution of the flare to the optical band is negligible, thus ruling out an internal shock origin for the optical emission and confirming that the optical emission represents the afterglow at the time of the RINGO measurement.

Although the optical emission from GRB 060418 was bright at an early time, no dominant optical flash from the reverse shock was detected, similar to other recently studied bright bursts such as GRB 061007 (*25*). The apparent lack of an optical or IR flash is easily explained in the standard fireball model if the typical synchrotron frequency of the forward-shock emission, ν_m, is lower than the observing frequency of the optical (and IR) band, ν_{opt}, at the onset of afterglow, or the peak time t_{peak}. This condition is required also to interpret the IR light-curve peak; otherwise, the rise gradient is expected to be shallower, $t^{1/2}$,

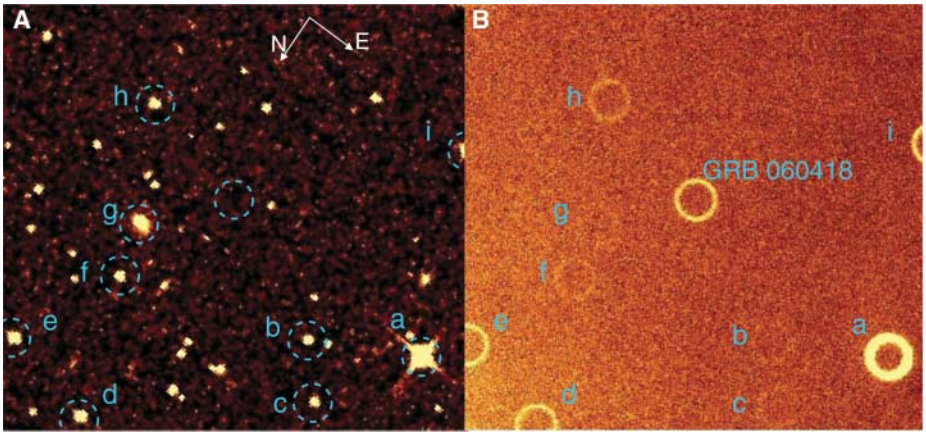

Fig. 1. Direct optical and RINGO polarimeter images of the field containing GRB 060418. The direct R-band image (**A**) is taken from the Digital Sky Survey (DSS) and shows the sky before the GRB occurred. The RINGO image (**B**) consists of a CCD recording of the incoming light from GRB 060418 and other bright sources in the field after the light has been modulated by a rotating polaroid and spread around rings by corotating deviating optics. The objects detected by RINGO are labeled (a) to (i) in both panels and blue dotted rings, corresponding to those in the RINGO image, are shown on the DSS image as a guide. All labeled objects, with the exception of extended object (g), are unresolved point sources and thus produce well-defined rings. The bright star (a) was used for additional calibration as described in the text. The field of view is 4.6 by 4.6 arc min, and the orientation of the field is shown by the white arrows indicating north (N) and east (E).

than observed (*26*). Mundell *et al*. (*25*) suggested that a low value of ν_m may be produced by small microphysics parameters, in particular low ϵ_B, due to small magnetic fields in forward and reverse shock regions. A low typical synchrotron frequency can also result if the fireball is enriched with electron-positron pairs. Nonstandard models of hydrodynamical jets with weak magnetic fields that radiate via inverse Compton emission, rather than synchrotron emission, have also been proposed as a mechanism for suppressing optical flashes. No polarization predictions for nonstandard models exist, so we do not discuss these models further. Instead, we test predictions from standard GRB models of relativistic jets with and without globally ordered magnetic fields that emit synchrotron radiation.

Theoretical models of magnetized jets, with large-scale ordered magnetic fields originating from the central engine, predict high values of polarization at very early times for the prompt γ-ray emission (*12*, *13*). Putative detections of large levels of γ-ray polarization of ~70 to 80% (*27*) and >35% and >50% (*28*) in a small number of GRBs provide support for large-scale ordered magnetic fields in the region of the flow that produces the high-energy prompt emission, but the observational results remain controversial (*29*). The optical emission from the forward shock is also predicted to be highly polarized for these magnetized jets; instabilities in the contact discontinuity at the fireball surface are expected to act as anchors for continuing the ordered magnetic field into the afterglow emission, producing optical polarization as high as 10 to 50% at an early time (*11*–*13*, *30*). The exact level of observed polarization depends on complex details of the degree of mixing between the ordered magnetic field in the ejecta and any tangled component in the shock front. Nevertheless, the key characteristic of emission from jets with large-scale ordered magnetic fields is that the observed polarization does not disappear at very early times (*13*).

Our robust upper limit $P < 8\%$ at the very early time $t \sim 203$ s for GRB 060418 lies below predicted values for reasonable jet properties. In the standard synchrotron shock model, the temporal decay rate of the optical afterglow, α, is related to the underlying power-law distribution of electron energies, or $dn/de = e^{-p}$; for GRB 060418, we derive $p = 2.6$, typical of optical afterglow emission. Theoretical models of a magnetically dominated flow for $p = 2.6$ predict observable polarization of a few tens of percent (*8*), substantially larger than that observed for GRB 060418. Within the limitations of current theoretical models, the low level of polarization observed in GRB 060418 therefore indicates that large-scale ordered magnetic fields are not dominant in the afterglow emission at early times.

Although reverse-shock emission in the form of an optical flash does not dominate the light curves of GRB 060418, in the hydrodynamic jet model more than ~50% of the emitted photons come from the original fireball material (*25*), or reverse-shock region, at the deceleration time when our polarization measurement of GRB 060418 was made. This is because at the peak time, the two shock emissions have the same cooling frequency, and the peak values of νF_ν at the cooling frequency are comparable. The two emissions contribute equally to the total flux at observing frequencies between the cooling frequency and the typical frequency of the forward shock (*24*), as is the case for optical measurements of GRB 060418.

We therefore rule out the presence of a magnetic field with ordered large-scale structure in a hydrodynamic or baryonic jet, in which the energy density of any magnetic field component is comparable to or less than that of the baryonic component, because this would also result in a large amount of polarization at an early time.

Our result is consistent with the theoretical prediction of low or zero polarization for hydrodynamical jets without large-scale ordered magnetic fields when observed at early times (*13*). This is also consistent with the reported lack of linear or circular polarization at radio frequencies for the afterglow of GRB 991216, observed at $t \sim 1$ day after the burst (*31*). Thus, we support models of hydrodynamical jets in which the generation of the magnetic field in the regions responsible for both the prompt and afterglow emission is driven by local processes in the fluid.

References and Notes

1. T. Piran, *Rev. Mod. Phys.* **76**, 1143 (2004).
2. P. Meszaros, *Rep. Prog. Phys.* **69**, 2259 (2006).
3. D. A. Frail *et al.*, *Astrophys. J.* **562**, L55 (2001).
4. T. Piran, *AIP Conf. Proc.* **784**, 164 (2005).
5. M. Lyutikov, *N. J. Phys.* **8**, 119 (2006).
6. A. Gruzinov, E. Waxman, *Astrophys. J.* **511**, 852 (1999).
7. G. Drenkhahn, H. C. Spruit, *Astron. Astrophys.* **391**, 1141 (2002).
8. M. Lyutikov, V. I. Pariev, R. D. Blandford, *Astrophys. J.* **597**, 998 (2003).
9. J. A. Nousek *et al.*, *Astrophys. J.* **642**, 389 (2006).
10. B. Zhang *et al.*, *Astrophys. J.* **642**, 354 (2006).
11. J. Granot, A. Königl, *Astrophys. J.* **594**, L83 (2003).
12. E. M. Rossi, D. Lazzati, J. D. Salmonson, G. Ghisellini, *Mon. Not. R. Astron. Soc.* **354**, 86 (2004).
13. D. Lazzati *et al.*, *Astron. Astrophys.* **422**, 121 (2004).
14. D. Bersier *et al.*, *Astrophys. J.* **583**, L63 (2003).
15. S. Covino *et al.*, *Astron. Astrophys.* **348**, 1 (1999).
16. J. Greiner *et al.*, *Nature* **426**, 157 (2003).
17. S. Covino *et al.*, *Astron. Astrophys.* **392**, 865 (2002).
18. A. J. Barth *et al.*, *Astrophys. J.* **584**, L47 (2003).
19. N. Gehrels *et al.*, *Astrophys. J.* **611**, 1005 (2004).
20. A. D. Falcone *et al.*, *GCN Circ*, 5009 (2006).
21. Materials and methods are available as supporting material on *Science* Online.
22. E. Molinari *et al.*, http://arxiv.org/abs/astro-ph/0612607 (2006).
23. S. Kobayashi, T. Piran, R. Sari, *Astrophys. J.* **513**, 669 (1999).
24. S. Kobayashi, B. Zhang, *Astrophys. J.* **582**, L75 (2003).
25. C. G. Mundell *et al.*, *Astrophys. J.* **660**, 1 (2007).
26. R. Sari, T. Piran, R. Narayan, *Astrophys. J.* **497**, L17 (1998).
27. W. Coburn, S. E. Boggs, *Nature* **423**, 415 (2003).
28. D. R. Willis *et al.*, *Astron. Astrophys.* **439**, 245 (2005).
29. R. E. Rutledge, D. B. Fox, *Mon. Not. R. Astron. Soc.* **350**, 1288 (2004).
30. A. Sagiv, E. Waxman, A. Loeb, *Astrophys. J.* **615**, 366 (2004).
31. J. Granot, G. B. Taylor, *Astrophys. J.* **625**, 263 (2005).

32. We thank S. Covino for useful discussions during the initial stages of the RINGO project. RINGO is a Liverpool Telescope fast-track instrument internally funded by the Astrophysics Research Institute of Liverpool John Moores University. The Liverpool Telescope is operated on the island of La Palma, the Canary Islands, by Liverpool John Moores University at the Observatorio del Roque de los Muchachos of the Instituto de Astrofisica de Canarias. C.G.M. thanks the Royal Society for financial support.

Supporting Online Material

www.sciencemag.org/cgi/content/full/1138484/DC1
Materials and Methods
Figs. S1 to S4
References and Notes

6 December 2006; accepted 2 March 2007
Published online 15 March 2007;
10.1126/science.1138484
Include this information when citing this paper.

Ballistic Electron Microscopy of Individual Molecules

Amin Bannani, Christian Bobisch, Rolf Möller*

We analyzed the transport of ballistic electrons through organic molecules on uniformly flat surfaces of bismuth grown on silicon. For the fullerene C_{60} and for a planar organic molecule (3,4,9,10-perylene-tetracarboxylic acid dianhydride), the signals revealed characteristic submolecular patterns that indicated where ballistic transport was enhanced or attenuated. The transport was associated to specific electronic molecular states. At electron energies of a few electron volts, this "scanning near-field electron transmission microscopy" method could be applied to various adsorbates or thin layers.

Future developments in microelectronics require a reduction in device size, ideally to one molecule, but the power dissipation of the individual element must be reduced accordingly. As demonstrated for silicon-based prototypes (*1*) as well as for carbon nanotubes (*2*), one route to such devices makes use of ballistic electron transistors. In the case of ballistic transport, the flow of electrons is not impeded by scattering at defects, so high speed and minimal energy loss are achieved. Ballistic transport has also been used to image surfaces.